Effect of water chemistry on the hydro-mechanical behaviour of compacted mixtures of claystone and Na + /Ca 2+ bentonites for deep geological repositories for deep geological repositories

Zhixiong Zeng, Yu-Jun Cui, Jean Talandier

▶ **To cite this version:**

Zhixiong Zeng, Yu-Jun Cui, Jean Talandier. Effect of water chemistry on the hydro-mechanical behaviour of compacted mixtures of claystone and Na + /Ca 2+ bentonites for deep geological repositories for deep geological repositories. Journal of Rock Mechanics and Geotechnical Engineering, 2022, 14 (2), pp.527-536. 10.1016/j.jrmge.2021.09.016 . hal-04181887

HAL Id: hal-04181887
https://enpc.hal.science/hal-04181887

Submitted on 16 Aug 2023

HAL is a multi-disciplinary open access archive for the deposit and dissemination of scientific research documents, whether they are published or not. The documents may come from teaching and research institutions in France or abroad, or from public or private research centers.

L'archive ouverte pluridisciplinaire **HAL**, est destinée au dépôt et à la diffusion de documents scientifiques de niveau recherche, publiés ou non, émanant des établissements d'enseignement et de recherche français ou étrangers, des laboratoires publics ou privés.

Effect of water chemistry on the hydro-mechanical behaviour of compacted mixtures of claystone and Na^+/Ca^{2+} bentonites for deep geological repositories

for deep geological repositories

Zhixiong Zeng[1*], Yu-Jun Cui[1], Jean Talandier[2]

1: Ecole des Ponts ParisTech, Laboratoire Navier/CERMES, 6 et 8 avenue Blaise Pascal, 77455 Marne La Vallée cedex 2, France
2: Andra, 1/7, rue Jean Monnet, 92298 Châtenay-Malabry cedex, France

Corresponding author

Zhixiong Zeng

Ecole des Ponts ParisTech
6–8 av. Blaise Pascal, Cité Descartes, Champs-sur-Marne
77455 Marne–la–Vallée cedex 2
France
Tel.: +33 781926608
Fax: +33 164153562
E-mail address: zhixiong.zeng@enpc.fr

Abstract: In the French deep geological disposal for radioactive wastes, compacted bentonite/claystone mixtures have been considered as possible sealing materials. After emplacement in place, such mixtures are hydrated by the site solution as well as the cement solution produced by the degradation of concrete. In this study, the effects of synthetic site solution and cement solution on the hydro-mechanical behaviour of compacted mixtures of claystone and two types of bentonites (Na^+ MX80 and Ca^{2+} Sardinia bentonites) were investigated by carrying out a series of swelling pressure, hydraulic conductivity and Mercury Intrusion Porosimetry (MIP) tests. It was found that for the MX80 bentonite/claystone mixture hydrated with synthetic site solution, the swelling capacity was reduced compared to the case with deionised water owing to the transformation of Na-montmorillonite to multi-cation dominant montmorillonite by cation exchanges. For the Sardinia bentonite/claystone mixture, the similar increasing rate of swelling pressure was observed during the crystalline swelling process for different solutions, suggesting insignificant cation exchanges. Additionally, the cations in the synthetic site solution could reduce the thickness of diffuse double layer and the osmotic swelling for both MX80 bentonite/claystone and Sardinia bentonite/claystone mixtures. The large-pore volume increased consequently and enhanced water flow. In the cement solution, the hydroxide could also dissolve the montmorillonite, reducing the swelling pressure, and increased the large-pore volume, facilitating the water flow. Furthermore, the decrease of swelling pressure and the increase of hydraulic conductivity were more significant in the case of low dry density because of more intensive interaction between montmorillonite and hydroxide thanks to the high permeability.

Keywords: bentonite/claystone mixture; synthetic site solution; cement solution; bentonite type; swelling pressure; hydraulic conductivity

1. Introduction

Deep geological repository has been accepted as a solution for the long-term storage of high-level radioactive wastes in many countries (Sellin and Leupin, 2013). To ensure the long-term safe isolation of radioactive wastes in deep geological formations, bentonite-based materials are commonly used as sealing materials (Pusch, 1982; Dixon et al., 1985; Villar and Lloret, 2008; Ye et al., 2010), while cement (in mortar or concrete) is used to construct the tunnel retaining structures and tunnel plugs/seals (Sánchez et al., 2006). After the repositories are closed, the bentonite-based materials will be hydrated by the pore water of the host rock and swell, filling the technological voids and restricting the release of radionuclides from the radioactive wastes to the surrounding environment. It has been reported that the pore water of the host rock considered in several countries is of certain salinity (Deng et al., 2011; Nguyen et al., 2013; Wang et al., 2014; Sun et al., 2018). In addition, the cement in contact with groundwater for a long period can degrade and release a large number of Ca^{2+} and OH^{-}, resulting in a high-pH alkaline solution (Savage et al., 2002; Karnland et al., 2007; Anh et al., 2017; Sun et al., 2018). In the performance assessment of the storage repositories, it appears essential to account for the effect of such water chemistry on the hydro-mechanical behaviour of bentonite-based materials.

In the past decades, the influence of saline solution on the hydro-mechanical behaviour of bentonite-based materials was studied by many researchers (Karnland et al., 2006; Rao et al., 2006; Castellanos et al., 2008; Komine et al., 2009; Zhu et al., 2013). It was found that the pore water salinity could significantly decrease the swelling pressure (Komine et al., 2009; Zhu et al., 2013) and increase the hydraulic conductivity (Castellanos et al., 2008; Zhu et al., 2013). Yukselen-Aksoy et al. (2008) and Zhu et al. (2013) reported that the cations in the pore water might alter the mineralogical

compositions through cation exchanges and influence the crystalline swelling process, resulting in a lower swelling pressure. Additionally, the cations in the pore water could decrease the thickness of diffuse double layer, affecting the osmotic swelling behaviour (Siddiqua et al., 2011; Castellanos et al., 2008; Schanz and Tripathy, 2009; Zhu et al., 2013; Du et al., 2021). At a given void ratio, a larger large-pore volume could be expected for the specimen hydrated with a saline solution, leading to a higher hydraulic conductivity.

In addition to the saline solution, alkaline solution can also significantly influence the hydro-mechanical behaviour of bentonite-based materials (Karnland et al., 2007; Herbert et al., 2008; Lee et al., 2012; Chen et al., 2016; Sun et al., 2018, 2019, 2020; Liu et al., 2020). Chen et al. (2016) experimentally determined the swelling pressures and hydraulic conductivities of GMZ bentonite hydrated with various NaOH solutions and found that the final swelling pressure decreased and the hydraulic conductivity increased significantly with the increase of NaOH solution concentration. Karnland et al. (2007) investigated the constant-volume swelling pressures of compacted Wyoming MX80 bentonite hydrated with NaOH and $Ca(OH)_2$ solutions and found that 0.1 M NaOH (pH=12.9) or saturated $Ca(OH)_2$ solutions (pH=12.4) did not significantly change the swelling pressure of compacted MX80 bentonite. In contrast, Sun et al. (2018; 2019) compared the swelling pressures and mineralogical compositions of GMZ bentonite hydrated with Beishan site solution (pH=8.5), young concrete water (pH=13) and evolved concrete water (pH=12) and observed a remarkably lower swelling pressure in the case of young concrete water. They explained this phenomenon by the dissolution of montmorillonite upon saturation with alkaline solutions and the formation of some less active zeolites and calcium hydrated silicates. Additionally, the montmorillonite content decreased linearly as the pH increased (Sun et al., 2019).

In France, Callovo-Oxfordian (COx) claystone has been considered as a potential geological host rock for high-level radioactive waste disposal. To reduce the excavation waste and ensure the mineralogical compatibility, a mixture of crushed COx claystone and bentonite in the form of pre-compacted blocks has been proposed as a possible sealing material by the French National Radioactive Waste Management Agency (Andra) (Wang e al., 2014; Zeng et al., 2019; Middelhoff, 2020). Wang et al. (2014) carried out a series of constant-volume swelling pressure tests on compacted MX80 bentonite/COx claystone mixture with a bentonite fraction of 70% (dry density of 1.7 Mg/m^3) and observed a slight decrease of swelling pressure with the synthetic site solution after 700 days of hydration. Cuisinier et al. (2009) studied the microstructure of compacted COx claystone at a dry density of 1.61 Mg/m^3 hydrated with portlandite-saturated solution for 1 year using mercury intrusion porosimetry (MIP) and scanning electron microscopy (SEM) techniques and found an increase of macro-pore void ratio after the fluid circulation. By contrast, Middelhoff (2020) indicated that the swelling pressure after about 7 days and the hydraulic conductivity after 1 year were hardly affected by the site solution and cement solution for the compacted MX80 bentonite/COx claystone mixture (a proportion of 30/70 in dry mass) at a dry density of 1.72 Mg/m^3. Up to now, there was no consensus regarding the effects of site solution and cement solution on the hydro-mechanical behaviour of bentonite/claystone mixture. Additionally, to the authors' knowledge, the responses of the mixtures of COx claystone and different bentonites upon hydration with site solution and cement solution have not been systematically studied.

In this study, a series of infiltration tests using deionised water, synthetic site solution and cement solution were performed on compacted mixtures of COx claystone and Na^+ MX80 and Ca^{2+} Sardinia bentonites at different dry densities. The effects of synthetic site solution and cement solution on the

swelling pressure and hydraulic conductivity were analysed. Moreover, the microstructure features before and after hydration were also determined using MIP technique, enabling the interpretation of the physico-chemical interaction between different bentonite/claystone mixtures and different fluids involved.

2. Materials and methods

2.1. Materials

According to the preliminary results of Zeng et al. (2020a), the bentonite/claystone mixtures with a proportion of 30/70 in dry mass were used in this study to fulfill the requirements of Andra in terms of swelling pressure and hydraulic conductivity with a dry density of 1.72-1.82 Mg/m^3. To investigate the effect of bentonite type, two bentonites, MX80 and Sardinia bentonites, were considered. The MX80 bentonite is a Na-bentonite, extracted from Wyoming in the United States while the Sardinia bentonite is a Ca-bentonite, taken from Monte Furros, Italy. The main physical and chemical characteristics of the two bentonites are presented in Table 1. The COx claystone was sampled from the Andra Underground Research Laboratory (URL) in Bure. It is composed of 40–45% interstratified illite/smectite, 30% carbonates, and 25%–30% quartz and feldspar. The COx claystone is characterized by a liquid limit of 41%, a plastic limit of 24% and a specific gravity of 2.70. Prior to testing, the bentonites and claystone were crushed to have a maximum grain size of 2.0 mm. The grain size distributions of the bentonites and claystone determined by dry sieving are presented in Fig. 1. The mean grain diameters (D_{50}) of the MX80 bentonite, Sardinia bentonite, COx claystone are 0.55, 1.06 and 0.58 mm, respectively.

Synthetic site solution and cement solution were used for the infiltration tests. These solutions respectively represent the site water at a depth of 490 m and the alkaline solution after the degradation

of concrete, and were prepared according to the recipe provided by Andra (Table 2). The chemical compositions of the solutions are summarized in Table 3. The pH values of the two solutions were measured, equal to 8.6 and 12.5, respectively. In addition, deionised water was also employed as a reference case.

2.2. Experimental methods

The bentonite and claystone powders with a proportion of 30/70 in dry mass were first mixed for more than 10 min. The gravimetric water contents of the MX80 bentonite, Sardinia bentonite and claystone under laboratory conditions (a relative humidity of about 60%) were determined by oven-drying at 105 °C for 24 h, equal to 11.4, 16.0 and 6.1%, respectively. Accordingly, the respective water contents of the MX80 bentonite/claystone and Sardinia bentonite/claystone mixtures were 7.7 and 9.1%, respectively. Based on the target dry density, a pre-determined amount of mixtures were poured into a rigid steel ring with an inner diameter of 50 mm and statically compacted at a constant displacement rate of 0.05 mm/min. The final height of compacted specimens was 10 mm. For the MX80 bentonite/claystone mixture, nine specimens with dry densities of 1.6, 1.8 and 2.0 Mg/m^3 were compacted, three for each dry density (Table 4); for the Sardinia bentonite/claystone mixture, six specimens with dry densities of 1.6 and 1.8 Mg/m^3 were prepared. Afterwards, the compacted specimens were transferred into a testing cell with an inner diameter of 50 mm (Fig. 2) and placed between two porous stones and filter papers. A circular cap with a diameter of 50 mm was placed at the top of the specimens and then blocked using a screw to prevent axial swelling. After that, deionised water, synthetic site solution or cement solution was injected into the specimens from the bottom of the cell under a water head of about 1 m and the axial swelling force was monitored using a force transducer installed under the testing cell. For all the specimens, the hydration lasted for 90

156 days. All the tests were performed at constant ambient temperature (20 ± 1 °C).

157 At the end of the swelling pressure tests, the solution injection was continued for more than 24
158 h using a pressure/volume controller under constant pressures. To minimise the disturbance of the
159 microstructure and avoid hydraulic fracturing, the water injection pressure was lower than 1/10 of the
160 final swelling pressure. For the MX80 bentonite/claystone mixtures at 1.6, 1.8 and 2.0 Mg/m^3 dry
161 densities, the injection pressures were respectively 0.04, 0.10 and 0.20 MPa, while those for the
162 Sardinia bentonite/claystone mixtures at 1.6 and 1.8 Mg/m^3 dry densities were 0.03 and 0.10 MPa,
163 respectively. During the solution injection, the solution volume injected into the specimens was
164 recorded. After stabilization of the flow rate, the specimens were regarded as saturated and the
165 saturated hydraulic conductivity was calculated based on the Darcy's law:

166 $$k=\frac{q}{iA} \quad (1)$$

167 where q is the flow rate (m^3/s); i is the hydraulic gradient; A is the cross-section (m^2).

168 After the infiltration tests, the specimens were taken out of the cell for microstructure
169 observation. The specimens were first cut into small pieces (about 1 cm^3 in volume). Afterwards, the
170 pieces were immersed in slush nitrogen (-210°C) obtained by previously submitting it to vacuum for
171 instantaneous freezing, and then lyophilized in a vacuumed chamber (Delage et al., 1996). For the
172 MIP test, the freeze-dried pieces were put in a low pressure chamber with a working pressure from
173 3.6 to 2000 kPa and then a high pressure chamber with a working pressure from 0.2 to 228 MPa,
174 enabling identification of pore entrance diameter 350 to 0.006 μm (the diameter at the narrowest
175 position).

176 **3. Experimental results**

177 *3.1. Swelling pressure*

178 The evolutions of swelling pressure for different dry densities are depicted in Fig. 3. On the whole,
179 the curves can be divided into two stages: a relatively large primary swell (stage I) and a small
180 secondary swell (stage II). In stage I, the swelling pressure increased quickly. The overall increasing
181 rate for the MX80 bentonite/claystone mixture hydrated with synthetic site solution and cement
182 solution was slightly lower than that of the specimens hydrated with deionised water. Moreover, the
183 synthetic site and cement solutions reduced the elapsed time required to complete stage I. By contrast,
184 the increasing rate for the Sardinia bentonite/claystone mixture was almost the same regardless of the
185 permeating solutions. In stage II, for the MX80 bentonite/claystone mixture with large dry densities
186 (1.8 and 2.0 Mg/m^3), the swelling pressure tended to stabilization. By contrast, for the MX80
187 bentonite/claystone mixture at a low dry density (1.6 Mg/m^3) and the Sardinia bentonite/claystone
188 mixtures at dry densities of 1.6 and 1.8 Mg/m^3, the swelling pressure reached a peak, decreased
189 sharply and then tented to stabilization. The specimens at a low dry density and hydrated with cement
190 solution exhibited a more remarkable decrease of swelling pressure after reaching a peak. Moreover,
191 at a given dry density, the decrease of swelling pressure after reaching a peak was more significant
192 for the Sardinia bentonite/claystone mixture compared to the MX80 bentonite/claystone mixture. The
193 final swelling pressures of the specimens at various dry densities and hydrated with different solutions
194 are summarized in Fig. 4. There were reasonable linear relationships between the final swelling
195 pressure and the dry density for the specimens hydrated with different solutions. In case of high dry
196 densities (1.8 and 2.0 Mg/m^3), the final swelling pressure was almost independent of the permeating
197 solution. In case of low dry density (1.6 Mg/m^3), the synthetic site solution and cement solution more
198 or less reduced the swelling pressure. Additionally, from Fig. 4, a slightly lower final swelling
199 pressure could be observed on the Sardinia bentonite/claystone mixture comparted to the MX80

bentonite/claystone mixture, especially in the case of low dry density of 1.6 Mg/m^3.

3.2. Saturated hydraulic conductivity

At the end of swelling pressures tests, the saturated hydraulic conductivities were determined for various dry densities and the results are presented in Fig. 5. For the specimens hydrated with a given solution, the hydraulic conductivity decreased with the increase of dry density. The synthetic site solution and cement solution increased the hydraulic conductivity for both the MX80 bentonite/claystone and the Sardinia bentonite/claystone mixtures. This is consistent with the results of Villar (2006) and Chen et al. (2016) while studying the effects of saline and alkaline solutions on the hydraulic conductivity of MX80 bentonite/granite mixture (a proportion of 30/70 in dry mass) and GMZ bentonite, respectively. Additionally, larger increases of hydraulic conductivity due to the water chemistry were observed on the specimens hydrated with cement solution. The lower the dry density of specimens, the more significant the influences of synthetic site solution and cement solution on the saturated hydraulic conductivity. In addition, compared to the MX80 bentonite/claystone mixture, the compacted Sardinia bentonite/claystone mixture exhibited a larger hydraulic conductivity at the same dry density.

3.3. Microstructure observation

Figs. 6 and 7 illustrate the pore size distributions of the specimens before and after hydration. From the cumulative curves (Figs. 6a and 7a), it could be observed that the final value of intruded mercury void ratio was lower than the global void ratio. This difference indicated the existence of a large amount of porosity which was inaccessible with the maximum pressure applied in the MIP tests. From the density curves (Figs. 6b and 7b), the as-compacted specimens exhibited a typical bimodal porosity, allowing two main pore populations to be defined: a population of intra-aggregate pores (small pores)

with a mean pore diameter of 0.02 μm and a population of inter-aggregate pores (large pores) with a mean pore diameter of 5 μm. This is consistent with the observation of Delage et al. (1996; 2006) who found that the soils compacted dry of optimum could be described by a typical aggregate microstructure. After hydration, the mean pore diameter of large pores increased to about 25 μm. By contrast, the mean pore diameter of small pores remained unchanged but the peak value decreased remarkably. For the specimens at low dry densities (1.6 and 1.8 Mg/m^3), a new pore population with a mean diameter of 0.2-0.5 μm (defined as medium pores) appeared between the large and small pores. Following the suggestion of Bian et al. (2019) and Zeng et al. (2020b), the respective delimiting diameters between the large and medium pores and between the medium and small pore were taken as 2 and 0.04 μm, respectively. To further investigate the effects of synthetic site solution and cement solution on the pore structure of bentonite/claystone mixtures, the void ratios of four populations were determined based on the delimiting values and the cumulative curves. The results are summarized in Figs. 8 and 9. It can be clearly observed that the synthetic site solution and cement solution increased the larger-pore and small-pore void ratios and decreased the medium-pore void ratio. Similar phenomenon was observed by Wang et al. (2014) and Liu et al. (2020) while investigating the effect of saline solution on the pores structure of compacted MX80 bentonite/claystone (70/30 in dry mass) and the effect of NaOH solution on the pore structure of compacted GMZ bentonite, respectively. Moreover, the cement solution had a more remarkable influence on the pore structure changes than the synthetic site solution. Comparison of the pore structures of two bentonite/claystone mixtures shows that at a given dry density, the Sardinia bentonite/claystone mixture exhibited a lower large-pore void ratio and larger medium-pore and small-pore void ratios than the MX80 bentonite/claystone mixture.

4. Interpretation and discussion

4.1. Effects of synthetic site solution and cement solution on hydro-mechanical behaviour

When the clay minerals in the bentonite/claystone mixtures were wetted with water, their hydration could be described by crystalline and osmotic swelling processes (Mitchell, 1993). At a low relative humidity, crystalline hydration is the predominant mechanism with water molecules being progressively adsorbed on the clay surfaces layer by layer, leading to an increase of the intra-aggregate pore volume. Meanwhile, the swollen aggregates invaded the inter-aggregate pores and reduced the inter-aggregate-pore volume. Obviously, this process depended on the global dry density. The lower the dry density, the more significant the swelling of aggregates. With the transformation of intra-aggregate and inter-aggregate pores to the medium-pore population, a remarkable increase of medium-pore void ratio occurred (Figs. 8 and 9). During the crystalline swelling process, the clay particles would be divided into smaller ones and fissure-like 2-dimensional (2-D) pores with a mean pore size of 20 μm appeared. The variation of large-pore volume after hydration was due to the combined effects of the invasion of swollen clay particles and the appearance of 2-D pores. As the suction decreased down to 4 MPa, the crystalline swelling reached a nearly steady state and a significant amount of water would be stored in inter-particle pores (Saiyouri et al., 2000). Due to the difference of cation concentration between the pore water and the clay particle surface, diffuse double layer would develop on a parallel assembly of clay particles (Liu, 2013) and osmotic swelling took place.

Generally, the maximum number of water molecule layers intercalated between the unit layers depends on the clay type and the available cations in the permeating water (Marcial et al., 2002; Liu, 2013). If the cation in the pore water is characterized by a high replacing power, cation exchanges can take place and the clay type will change. A typically competitive order that has been commonly

admitted is: Na^+<K^+<Mg^{2+}<Ca^{2+} (Mitchell, 1993; Mata, 2003; Sun et al., 2018). As shown in Table 3, the synthetic site solution and cement solution used in this study contain a certain amount of K^+, Mg^{2+} or Ca^{2+} cations. According to the X-Ray diffractometry (XRD) results on GMZ bentonite by Sun et al. (2019), Na-montmorillonite would be transformed to Mg/Ca- dominant montmorillonite and Ca- dominant montmorillonite after the interaction with synthetic site solution and cement solution, respectively. During the crystalline swelling process, the water adsorption capacity of Na-montmorillonite was larger than that for Ca-montmorillonite (Liu, 2013; Du et al., 2020; Yotsuji et al., 2021). Therefore, this transformation of Na-montmorillonite would decrease the swelling capacity of the montmorillonite. Additionally, as the cation concentration of pore water increased, the repulsive force between the diffuse double layer and the thickness of the diffuse double layer decreased (Yong and Warkentin, 1975; Mitchell, 1976). Consequently, a lower swelling pressure was observed for the specimens hydrated with synthetic site solution (Fig. 4). At a given global void ratio, this decreased distance between clay particles leads to an increase of the large-pore void ratio. As a result, a larger hydraulic conductivity was observed for the specimens hydrated with synthetic site solution (Fig. 5) (Cuisinier et al., 2011).

Apart from the cations, the hydroxide in the cement solution can also greatly influence the hydro-mechanical behaviour of the bentonite/claystone mixtures. Upon contact with hydroxide, the montmorillonite might be dissolved, forming secondary minerals with much lower swelling capacity, such as analcime and calcium hydrated silicates gels (Sun et al., 2018; 2019). As result, the swelling capacity was reduced (Fig. 4). The produced calcium hydrated silicates gels were characterized by a large amount of small pores (Wang et al., 2017), leading to an increase of small-pore void ratio of the specimens hydrated with cement solution (Figs. 8 and 9) (Sun et al., 2019; Liu et al., 2020). By

289 contrast, the dissolution of montmorillonite would lead to an increase of the large-pore volume (Chen
290 et al., 2016). Compared to the specimens hydrated with synthetic site solution, the specimens could
291 be affected by the hydroxide in addition to the cations. Thus, the specimens hydrated with cement
292 solution exhibited a larger large-pore volume and a higher hydraulic conductivity compared with
293 those hydrated with synthetic site solution (Fig. 5).

294 *4.2. Effects of bentonite type and dry density on hydro-mechanical behaviour*

295 Basically, the synthetic site solution and cement solution can influence the hydro-mechanical
296 behaviour of bentonite-based materials mainly by means of cation exchanges, osmotic effect and
297 montmorillonite dissolution. After the MX80 bentonite/claystone and Sardinia bentonite/claystone
298 mixtures were in contact with synthetic site solution, cation exchanges could occur in the MX80
299 bentonite/claystone mixture, with the transformation of some Na-montmorillonite to Mg-, and Ca-
300 montmorillonite, while the Sardinia bentonite/claystone mixture would be immune to the cation
301 exchange. This would reduce the swelling capacity of MX80 bentonite/claystone mixture. Thus, a
302 slightly smaller increasing rate of swelling pressure for this mixture in stage I for MX80
303 bentonite/claystone mixture, as compared to that hydrated with deionised water (Fig. 3a and b).
304 Thanks to the higher permeability, the interaction between clay minerals and solution became more
305 intensive for the MX80 bentonite/claystone mixture at a lower dry density upon the hydration with
306 the synthetic site solution. By contrast, the cations in the synthetic site solution would exert an
307 influence on the osmotic swelling of both the MX80 bentonite/claystone and the Sardinia
308 bentonite/claystone mixtures at low dry densities. In general, the clay particles of Na-montmorillonite
309 after crystalline swelling are thinner than those of Ca-montmorillonite (Saiyouri et al., 2004). It was
310 reported that the clay particles are composed of 2–20 (and even more) aligned unit layers in Ca-

311 montmorillonite, but only of 1–5 unit layers in Na-montmorillonite (Liu, 2013). Therefore, during the
312 osmotic swelling process, few double layer development could be expected in the Ca-montmorillonite,
313 as compared to the Na-montmorillonite. The weaker osmotic swelling of Sardinia bentonite/claystone
314 mixture could not compensate the reduction of swelling pressure induced by the collapse of aggregate
315 structure. Thus, a more significant decrease was observed in stage II at low dry densities (Fig. 3a and
316 b). Additionally, the cations in the synthetic site solution could reduce the repulsive force and the
317 thickness of diffuse double layer, resulting in a lower swelling pressure and a higher hydraulic
318 conductivity for the specimens hydrated with synthetic site solution (Figs. 4 and 5). For the specimens
319 at high dry densities, the low amount of inter-particle water was insufficient to form the diffuse double
320 layer (Pusch and Yong, 2006) and the effect of cations on the swelling pressure and hydraulic
321 conductivity of the highly compacted MX80 bentonite/claystone and Sardinia bentonite/claystone
322 mixtures was less significant.

323 **5. Conclusions**

324 The effects of synthetic site solution and cement solution on the hydro-mechanical behaviour of
325 compacted Na^+ MX80 bentonite/claystone and Ca^{2+} Sardinia bentonite/claystone mixtures were
326 investigated by carrying out a series of swelling pressure and hydraulic conductivity tests together
327 with microstructure observation. The results obtained allow the following conclusions to be drawn:

328 For the MX80 bentonite/claystone mixture, the cations in synthetic site solution could transform
329 the Na-montmorillonite to multi-cation dominant montmorillonite, reducing the swelling capacity
330 of the mixture. By contrast, for the Sardinia bentonite/claystone mixture, the cations in synthetic site
331 solution did not significantly change the Ca-montmorillonite during the crystalline swelling. Thus,
332 an insignificant effect was identified on the swelling pressure.

During the osmotic swelling, the presence of cations reduced the repulsive force by diffuse double layer and thus swelling pressure for both the MX80 bentonite/claystone and Sardinia bentonite/claystone mixtures. Additionally, a smaller thickness of diffuse double layer and a greater large-pore volume could be expected for the specimens hydrated with synthetic site solution. Thus, a slightly higher saturated hydraulic conductivity was obtained in that case, as compared to the case of deionised water. Furthermore, a more significant influence of synthetic site solution was observed on the specimens at a lower dry density thanks to the well-developed diffuse double layer.

In addition to the cations, the hydroxide also reduced the swelling pressure of both the MX80 bentonite/claystone and Sardinia bentonite/claystone mixtures. The hydroxide led to a slight increase of large-pore volume and thus an increase of saturated hydraulic conductivity. Moreover, the lower the dry density, the more intensive the interaction between the montmorillonite and hydroxide and the more significant the changes in swelling pressure and hydraulic conductivity, due to the higher permeability.

Over the experiment time scale of 90 days, only a slight deterioration of sealing performance of the bentonite/claystone mixture was identified due to the low cation concentration and the low ionic strength of permeating solutions. The effect of water chemistry in the very long-term lifespan of the underground radioactive waste repository needs to be investigated in further work.

Acknowledgments

The research work was supported by Ecole des Ponts ParisTech and the French National Radioactive Waste Management Agency (Andra). The first author is grateful to the China Scholarship Council for the grant scholarship.

355 **References**

356 Anh, H.N., Ahn, H., Jo, H.Y., Kim, G.Y., 2017. Effect of alkaline solutions on bentonite properties.
357 Environmental Earth Sciences, 76(10), 374.

358 Bian, X., Cui, Y.J., Li, X.Z., 2019. Voids effect on the swelling behaviour of compacted bentonite.
359 Géotechnique, 69(7), 593-605.

360 Cara, S., Carcangiu, G., Padalino, G., Palomba, M., Tamanini, M., 2000. The bentonites in
361 pelotherapy: chemical, mineralogical and technological properties of materials from Sardinia
362 deposits (Italy). Applied Clay Science, 16(1-2), 117-124.

363 Castellanos, E., Villar, M.V., Romero, E., Lloret, A., Gens, A., 2008. Chemical impact on the hydro-
364 mechanical behaviour of high-density FEBEX bentonite. Physics and Chemistry of the Earth,
365 Parts A/B/C 33, S516-S526.

366 Chen, B., Guo, J.X., Zhang, H.X., 2016. Alteration of compacted GMZ bentonite by infiltration of
367 alkaline solution. Clay Minerals, 51(2), 237-247.

368 Cuisinier, O., Deneele, D., Masrouri, F., 2009. Shear strength behaviour of compacted clayey soils
369 percolated with an alkaline solution. Engineering geology, 108(3-4), 177-188.

370 Cuisinier, O., Auriol, J.C., Le Borgne, T., Deneele, D., 2011. Microstructure and hydraulic
371 conductivity of a compacted lime-treated soil. Engineering geology, 123(3), 187-193.

372 Delage, P., Audiguier, M., Cui, Y.J., Howat, M.D., 1996. Microstructure of a compacted silt.
373 Canadian Geotechnical Journal, 33(1), 150-158.

374 Delage, P., Marcial, D., Cui, Y.J., Ruiz, X., 2006. Ageing effects in a compacted bentonite: a
375 microstructure approach. Géotechnique, 56(5), 291-304.

376 Deng, Y.F., Tang, A.M., Cui, Y.J., Nguyen, X.P., Li, X.L., Wouters, L., 2011. Laboratory hydro-

377 mechanical characterisation of Boom Clay at Essen and Mol. Physics and Chemistry of the Earth,
378 Parts A/B/C, 36(17-18), 1878-1890.
379 Dixon, D.A., Gray, M.N., Thomas, A.W., 1985. A study of the compaction properties of potential
380 clay-sand buffer mixtures for use in nuclear fuel waste disposal. Eng. Geol. 21(3/4): 247-255.
381 Du, J.P., Zhou, A.N., Lin, X., Bu, Y., Kodikara, J., 2020. Revealing expansion mechanism of cement-
382 stabilized expansive soil with different interlayer cations through molecular dynamics
383 simulations. The Journal of Physical Chemistry C, 124(27), 14672-14684.
384 Du, J.P., Zhou, A.N., Lin, X., Bu, Y., Kodikara, J., 2021. Prediction of swelling pressure of expansive
385 soil using an improved molecular dynamics approach combining diffuse double layer theory.
386 Applied Clay Science, 203, 105998.
387 Heikola, T., Kumpulainen, S., Vuorinen, U., Kiviranta, L., Korkeakoski, P., 2013. Influence of
388 alkaline (pH 8.3–12.0) and saline solutions on chemical, mineralogical and physical properties
389 of two different bentonites. Clay Minerals, 48(2), 309-329.
390 Herbert, H., Kasbohm, J., Sprenger, H., Fernández, A.M., Reichelt, C., 2008. Swelling pressures of
391 MX-80 bentonite in solutions of different ionic strength. Phys. Chem. Earth, 33, S327–S342.
392 Karnland, O., Olsson, S., Nilsson, U., 2006. Mineralogy and sealing properties of various bentonites
393 and smectite-rich clay materials. Technical Report No. TR-06-30. SKB, Swedish Nuclear Fuel
394 and Waste Management Co.
395 Karnland, O., Olsso, S., Nilsson, U., Sellin, P., 2007. Experimentally determined swelling pressures
396 and geochemical interactions of compacted Wyoming bentonite with highly alkaline solutions.
397 Phys. Chem. Earth, 32(1–7), 275–286.
398 Komine, H., Yasuhara, K., Murakami, S., 2009. Swelling characteristics of bentonites in artificial

399 seawater. Can. Geotech. J., 46, 177–189.
400 Lee, J.O., Lim, J.G., Kang, I.M., Kwon, S., 2012. Swelling pressures of compacted Cabentonite. Eng.
401 Geol. 129-130, 20–26.
402 Liu, L., 2013. Prediction of swelling pressures of different types of bentonite in dilute solutions.
403 Colloids and Surfaces A: Physicochemical and Engineering Aspects, 434, 303-318.
404 Liu, L.N., Chen, Y.G., Ye, W.M., Cui, Y.J., Wu, D.B., 2020. Swelling pressure deterioration of
405 compacted GMZ bentonite and its structural damage under heat combined with hyperalkaline
406 conditions. Geomechanics and Geoengineering, 1-12.
407 Mata, C., 2003. Hydraulic behaviour of bentonite based mixtures in engineered barriers: the Backfill
408 and Plug Test at the A ¨spo ¨HRL (Sweden). (Ph.D. Thesis) Universitat Polite'cnica de Catalunya,
409 Barcelona (257 pp.).
410 Marcial, D., Delage, P., Cui, Y.J., 2002. On the high stress compression of bentonites. Canadian
411 Geotechnical Journal, 39(4), 812-820.
412 Mitchell, J.K., 1976. Fundamentals o f Soil Behaviour. 1st edition. J. Wiley and Sons Publishers,
413 Toronto.
414 Mitchell, J.K., 1993. Fundamentals of soil behaviour, 2nd edn. John Wiley and sons, New York.
415 Middelhoff, M., 2020. Hydro-mechanical behavior of claystone-based backfill materials under geo-
416 environmental conditions. PhD thesis, Universit éde lorraine.
417 Nguyen, X.P., Cui, Y.J., Tang, A.M., Deng, Y.F., Li, X.L., Wouters, L., 2013. Effects of pore water
418 chemical composition on the hydro-mechanical behavior of natural stiff clays. Engineering
419 geology, 166, 52-64.
420 Pusch, R., 1982. Mineral–water interactions and their influence on the physical behavior of highly

421 compacted Na bentonite. Canadian Geotechnical Journal, 19(3): 381-387.
422 Pusch, R., Karnland, O., 1988. Geological evidence of smectite longevity: The Sardinian and Gotland
423 cases. Svensk kärnbränslehantering.
424 Pusch, R., Yong, R.N., 2006. Microstructure of smectite clays and engineering performance. CRC
425 Press.
426 Rao, S.M., Thyagaraj, T., Thomas, H.R., 2006. Swelling of compacted clay under osmotic gradients.
427 Géotechnique, 56(10), 707–713.
428 Saiyouri, N., Hicher, P.Y., Tessier, D., 2000. Microstructural approach and transfer water modelling
429 in highly compacted unsaturated swelling clays. Mechanics of Cohesive‐frictional Materials:
430 An International Journal on Experiments, Modelling and Computation of Materials and
431 Structures, 5(1), 41-60.
432 Saiyouri, N., Tessier, D., Hicher, P.Y., 2004. Experimental study of swelling in unsaturated
433 compacted clays. Clay minerals, 39(4), 469-479.
434 Sánchez, L., Cuevas, J., Ramírez, S., De León, D.R., Fernández, R., Villa, R.V.D., Leguey, S., 2006.
435 Reaction kinetics of FEBEX bentonite in hyperalkaline conditions resembling the cement–
436 bentonite interface. Applied Clay Science, 33(2), 125-141.
437 Savage, D., Noy, D., Mihara, M., 2002. Modelling the interaction of bentonite with hyperalkaline
438 fluids. Appl. Geochem. 17, 207–223.
439 Schanz, T., Tripathy, S., 2009. Swelling pressure of a divalent‐rich bentonite: Diffuse double‐
440 layer theory revisited. Water Resources Research, 45(5).
441 Sellin, P. Leupin, O.X., 2013. The use of clay as an engineered barrier in radioactive-waste
442 management–a review.Clays and Clay Minerals, 61(6), 477-498.

443 Siddiqua S, Blatz, J., Siemens, G., 2011. Evaluation of the impact of pore fluid chemistry on the
444 hydromechanical behavior of claybased sealing materials. Can Geothech J, 48, 199–213.
445 Sun, Z., Chen, Y.G., Cui, Y.J., Xu, H.D., Ye, W.M., Wu, D.B., 2018. Effect of synthetic water and
446 cement solutions on the swelling pressure of compacted Gaomiaozi (GMZ) bentonite: the
447 Beishan site case, Gansu, China. Engineering Geology, 244, 66-74.
448 Sun, Z., Chen, Y.G., Cui, Y.J., Ye, W.M., Chen, B., 2019. Effect of synthetic Beishan site water and
449 cement solutions on the mineralogy and microstructure of compacted Gaomiaozi (GMZ)
450 bentonite. Soils and Foundations, 59 (6), 2056-2069.
451 Sun, Z., Chen, Y.G., Ye, W.M., Cui, Y.J., Wang, Q., 2020. Swelling deformation of Gaomiaozi
452 bentonite under alkaline chemical conditions in a repository. Engineering Geology, 279, 105891.
453 Villar, M.V., 2006. Infiltration tests on a granite/bentonite mixture: Influence of water salinity.
454 Applied Clay Science, 31(1-2), 96-109.
455 Villar, M.V., Lloret, A. 2008. Influence of dry density and water content on the swelling of a
456 compacted bentonite. Appl. Clay Sci. 39(1–2), 38–49.
457 Vitale, E., Deneele, D., Russo, G., 2016. Multiscale analysis on the behaviour of a lime treated
458 bentonite. Procedia Engineering, 158, 87-91.
459 Wang, Q., Cui, Y.J., Tang, A.M., Delage, P., Gatmiri, B., Ye, W.M., 2014. Long-term effect of water
460 chemistry on the swelling pressure of a bentonite-based material. Applied clay science, 87, 157-
461 162.
462 Wang, Y., Duc, M., Cui, Y.J., Tang, A.M., Benahmed, N., Sun, W.J., Ye, W.M., 2017. Aggregate
463 size effect on the development of cementitious compounds in a lime-treated soil during curing.
464 Applied Clay Science, 136, 58-66.

Ye, W.M., Chen, Y.G., Chen, B., Wang, Q., Wang, J., 2010. Advances on the knowledge of the buffer/backfill properties of heavily-compacted GMZ bentonite. Engineering Geology, 116(1-2), 12-20.

Yong, R.N., Warkentin, B.P., 1975. Soil Properties and Behaviour. Elsevier, Amsterdam.

Yotsuji, K., Tachi, Y., Sakuma, H., Kawamura, K., 2021. Effect of interlayer cations on montmorillonite swelling: Comparison between molecular dynamic simulations and experiments. Applied Clay Science, 204, 106034.

Yukselen-Aksoy, Y., Kaya, A., Ören, A.H., 2008. Seawater effect on consistency limits and compressibility characteristics of clays. Eng. Geol., 102, 54–61.

Zeng, Z.X., Cui, Y.J., Zhang, F., Conil, N., Talandier, J., 2019. Investigation of swelling pressure of bentonite/claystone mixture in the full range of bentonite fraction. Applied Clay Science.

Zeng, Z., Cui, Y. J., Conil, N., Talandier, J., 2020a. Experimental Investigation and Modeling of the Hydraulic Conductivity of Saturated Bentonite–Claystone Mixture. International Journal of Geomechanics, 20(10), 04020184.

Zeng, Z., Cui, Y.J., Conil, N., Talandier, J., 2020b. Effects of technological voids and hydration time on the hydro-mechanical behaviour of compacted bentonite/claystone mixture. Géotechnique, 1-14.

Zhu, C.M., Ye, W.M., Chen, Y.G., Chen, B., Cui, Y.J., 2013. Influence of salt solutions on the swelling pressure and hydraulic conductivity of compacted GMZ01 bentonite. Eng. Geol., 166, 74–80.

List of Tables

List of Figures

511 **Table 1** Physical and chemical properties of MX80 and Sardinia bentonites

Soil property	MX80	Sardinia
Specific gravity	2.76	2.54[b]
Consistency limit		
Liquid limit (%)	494	143[b]
Plastic limit (%)	46	69[b]
Plasticity index (%)	448	74[b]
Cation exchange capacity (CEC) (meq/100 g)	80[a]	65[c]
Main minerals	Montmorillonite (86%)	Montmorillonite (60-90%)[d]
	Quartz (7%)	Illite (10-14%)[d]

512 a Karnland et al. (2006)

513 b Vitale et al. (2016)

514 c Cara et al. (2000)

515 d Pusch and Karnland (1988)

516 **Table 2** Recipe for the synthetic site solution and cement solution preparation

Content (g/L)	NaCl	$NaHCO_3$	KCl	$CaSO_4 \cdot 2H_2O$	$MgSO_4 \cdot 7H_20$	$CaCl_2 \cdot 2H_2O$	Na_2SO_4	$Ca(OH)_2$
Site solution	1.950	0.130	0.035	0.630	1.020	0.080	0.700	-
Cement solution	1.286	-	0.596	-	-	-	-	1.408

517

518 **Table 3** Composition of the synthetic site solution and cement solution

Compound (mmol/L)	Na^+	K^+	Ca^{2+}	Mg^{2+}	Cl^-	$SO4^{2-}$	CO_3^{2-}
Site solution	44.6	0.47	4.2	4.1	34.8	12.7	1.58
Cement solution	22.2	8.05	19	-	30.2	-	-

519

520 **Table 4** Experimental programme

Test No.	Bentonite type	Dry density (Mg/m^3)	Injected water	MIP
T01	MX80	1.6	Deionised water	√
T02	MX80	1.6	Site solution	√
T03	MX80	1.6	Cement solution	√
T04	MX80	1.8	Deionised water	√
T05	MX80	1.8	Site solution	√
T06	MX80	1.8	Cement solution	√
T04	MX80	2.0	Deionised water	√
T05	MX80	2.0	Site solution	√
T06	MX80	2.0	Cement solution	√
T04	Sardinia	1.6	Deionised water	√
T05	Sardinia	1.6	Site solution	√
T06	Sardinia	1.6	Cement solution	√
T04	Sardinia	1.8	Deionised water	√
T05	Sardinia	1.8	Site solution	√
T06	Sardinia	1.8	Cement solution	√

521

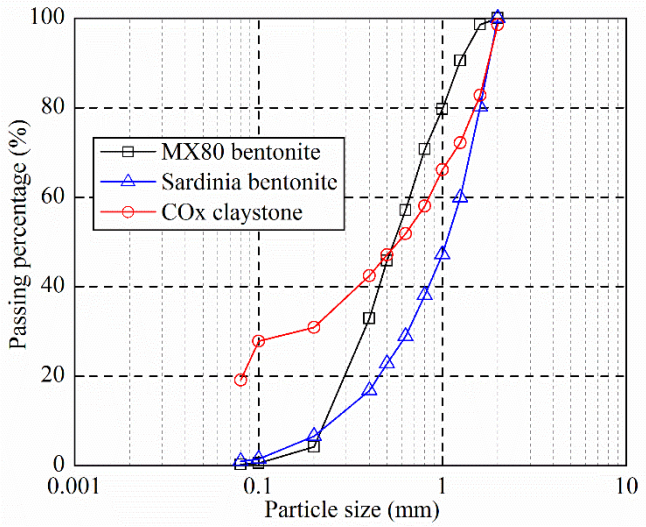

Fig. 1 Grain size distribution of MX80 and Sardinia bentonites and crushed COx claystone

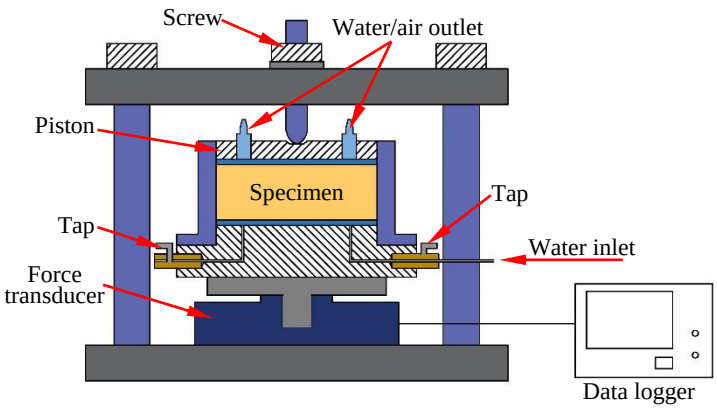

Fig. 2 Schematic diagram of the constant-volume cell for swelling pressure and hydraulic conductivity tests

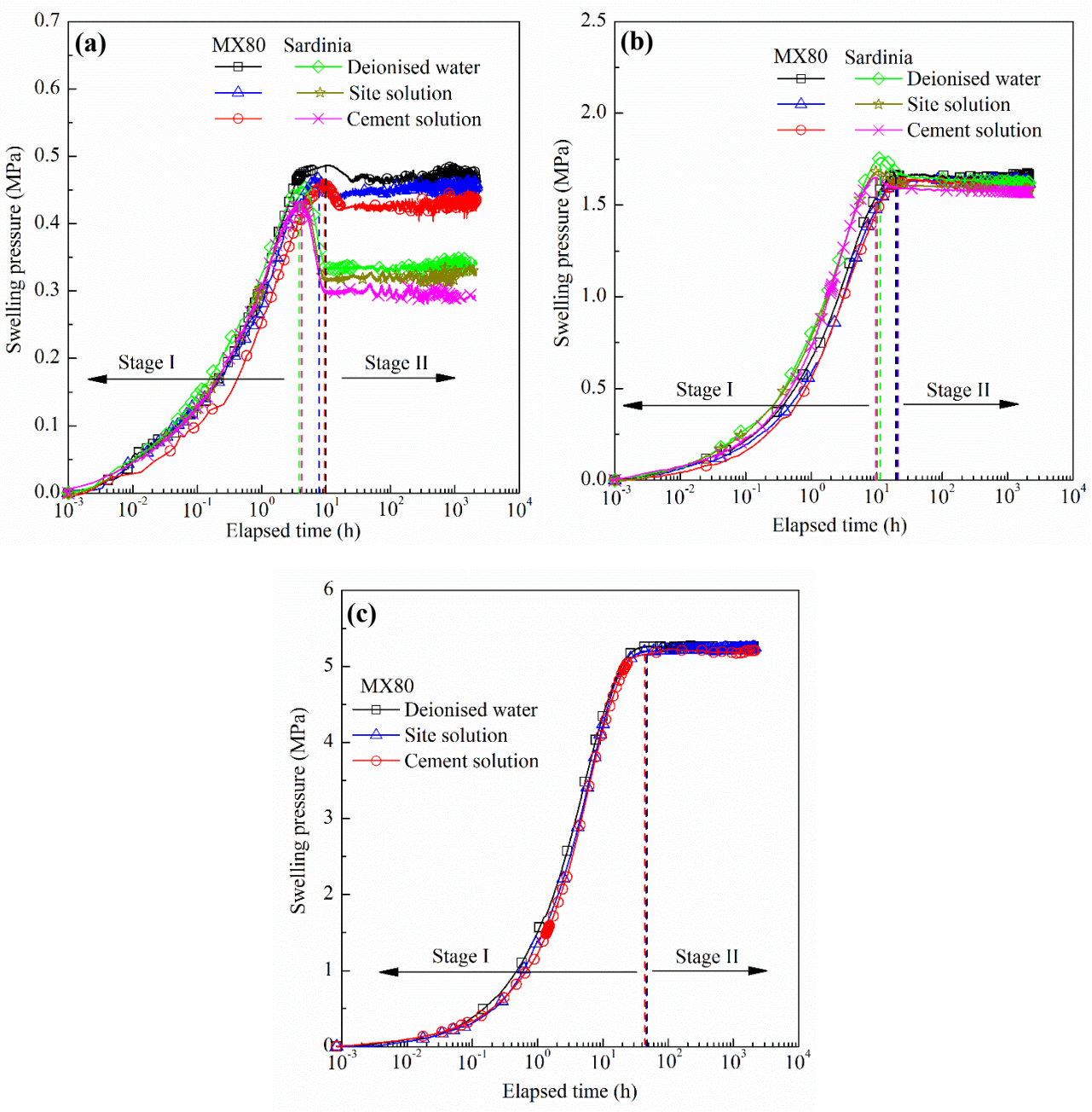

526

527

528 **Fig. 3** Evolution of axial swelling pressure of specimens at different dry densities. (a) 1.6 Mg/m^3, (b) 1.8 Mg/m^3 and (c) 2.0 Mg/m^3

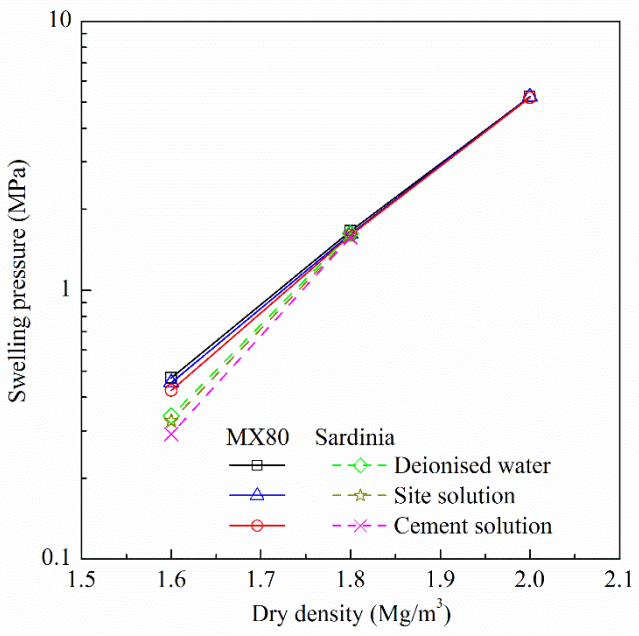

529
530

Fig. 4 Final swelling pressure versus dry density

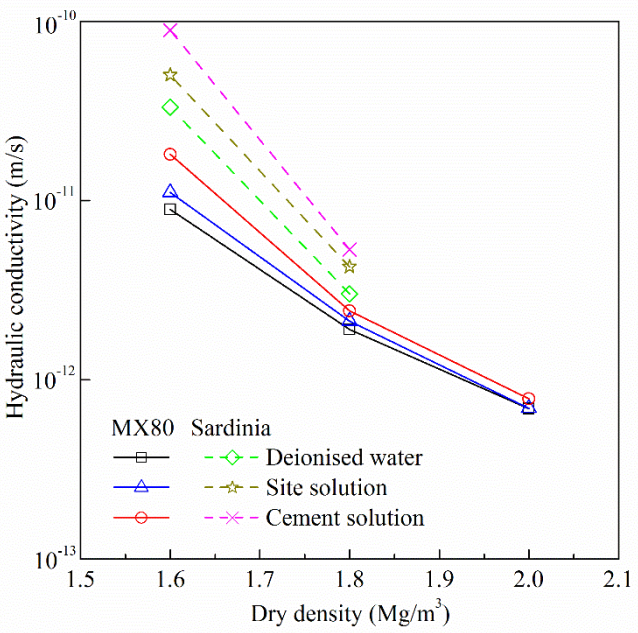

531
532

Fig. 5 Hydraulic conductivity versus dry density

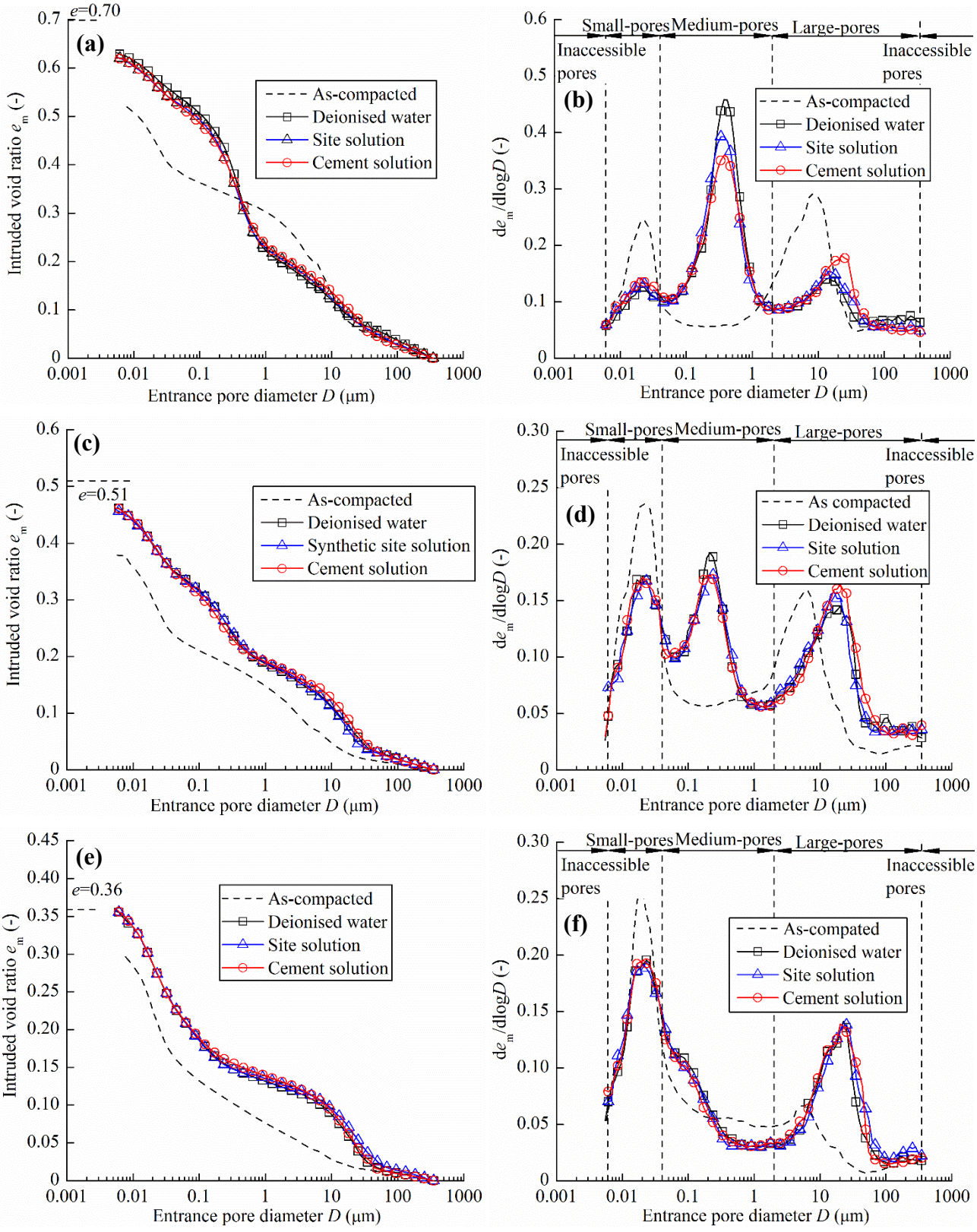

Fig. 6 Pore size distribution of MX80 bentonite/claystone mixtures: (a) cumulative curves of specimens at a dry density of 1.6 Mg/m^3, (b) density function curves of specimens at a dry density of 1.6 Mg/m^3, (c) cumulative curves of specimens at a dry density of 1.8 Mg/m^3, (d) density function curves of specimens at a dry density of 1.8 Mg/m^3, (e) cumulative curves of specimens at a dry density of 2.0 Mg/m^3 and (f) density function curves of specimens at a dry density of 2.0 Mg/m^3

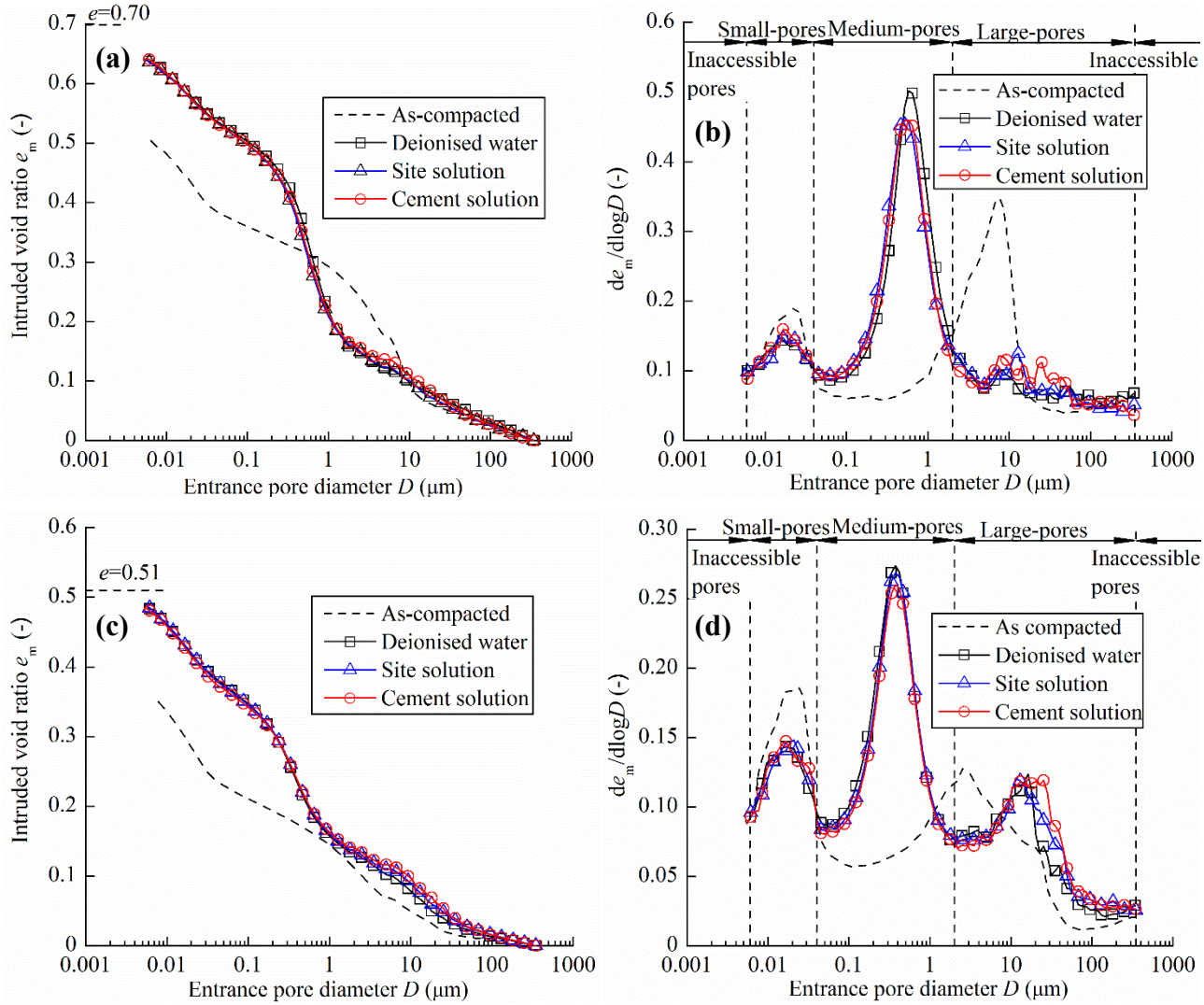

Fig. 7 Pore size distribution of Sardinia bentonite/claystone mixtures: (a) cumulative curves of specimens at a dry density of 1.6 Mg/m^3, (b) density function curves of specimens at a dry density of 1.6 Mg/m^3, (c) cumulative curves of specimens at a dry density of 1.8 Mg/m^3 and (d) density function curves of specimens at a dry density of 1.8 Mg/m^3

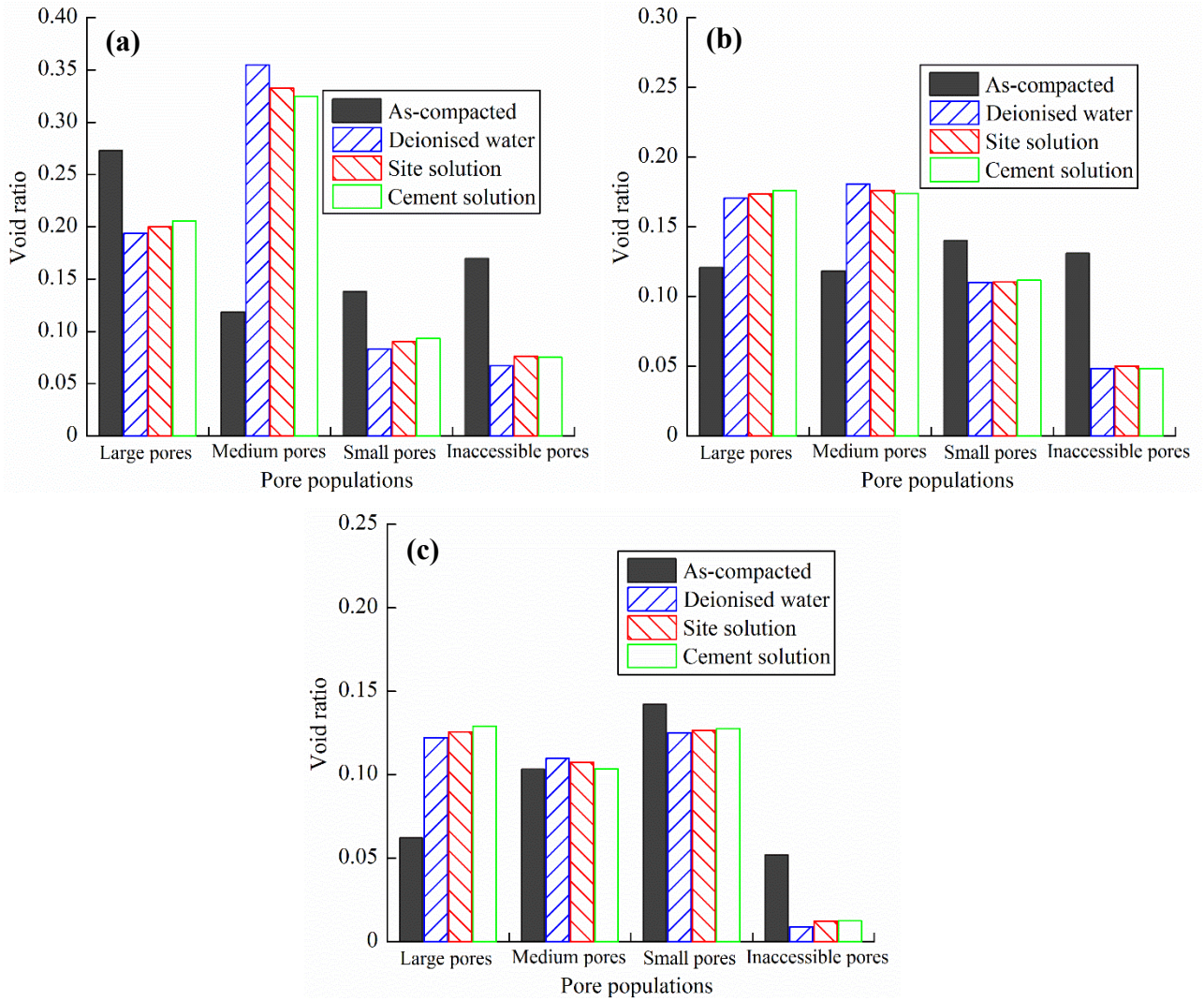

Fig. 8 Changes in inaccessible-pore, small-pore, medium-pore and large-pore void ratios for the compacted MX80 bentonite/claystone mixtures. (a) 1.6 Mg/m^3, (b) 1.8 Mg/m^3 and (c) 2.0 Mg/m^3

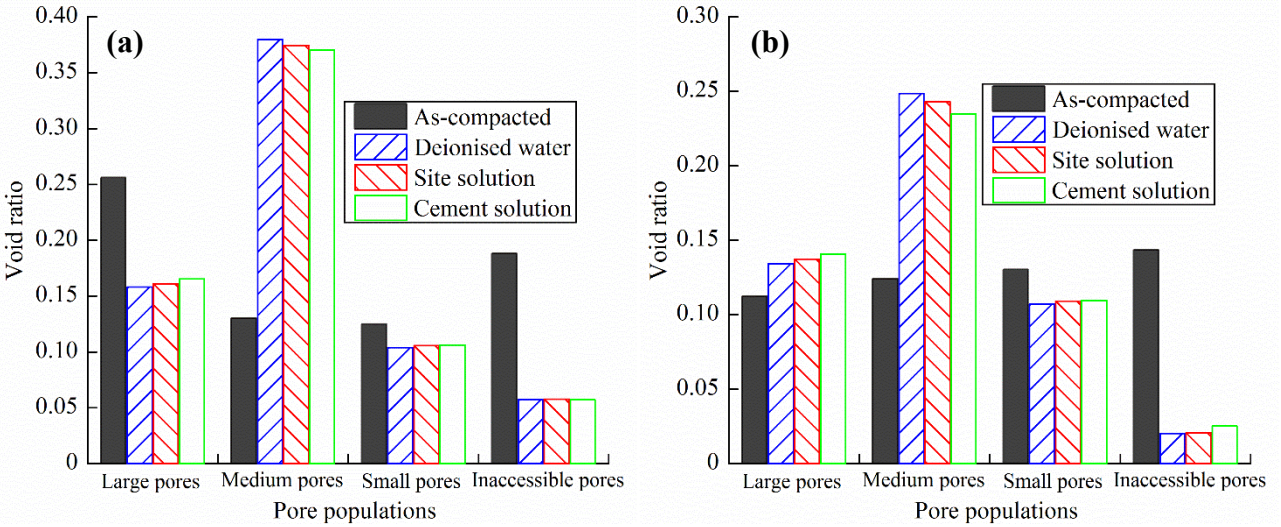

549
550 **Fig. 9** Changes in inaccessible-pore, small-pore, medium-pore and large-pore void ratios for the compacted Sardinia
551 bentonite/claystone mixtures. (a) 1.6 Mg/m^3 and (b) 1.8 Mg/m^3